

Plasma membrane cholesterol regulates the allosteric binding of 1-methyl-4-phenylpyridinium (MPP⁺) to organic cation transporter 2 (OCT2, SLC22A2)

Severin Hörmann, Zhibo Gai, Gerd A. Kullak-Ublick, Michele Visentin

Affiliations

Department of Clinical Pharmacology and Toxicology, University Hospital Zurich, University of Zurich, Switzerland (SH, ZG, GAK-U, MV)

Key Laboratory of Traditional Chinese Medicine for Classical Theory, Ministry of Education, Shandong University of Traditional Chinese Medicine, Jinan, China (ZG)

Mechanistic Safety, CMO & Patient Safety, Global Drug Development, Novartis Pharma, Basel, Switzerland (GAK-U)

Running Title

Cholesterol and OCT2- mediated transport

Corresponding author

Michele Visentin, Ph. D., University Hospital Zurich, Wagistrasse 14, CH-8952 Schlieren.

Phone: +41 445563148, Fax: +41 442554411, E-mail: Michele.visentin@usz.ch

Pages: 25

Tables: 1

Figures: 6

References: 56

Words Abstract: 218

Words Introduction: 468

Words Discussion: 913

Abbreviations

N-Methyl-4-phenylpyridinium acetate, MPP⁺; organic cation transporter, OCT; thin layer chromatography, TLC.

Section assignments: Metabolism, Transport and Pharmacogenomics

Keywords

Allosterism, cholesterol, lipid bilayer, methyl- β -cyclodextrin, tubular secretion

Abstract

The human organic cation transporter 2 (OCT2) mediates the first step of tubular secretion of most positively charged substances. The present work describes the role of plasma membrane cholesterol in OCT2 activity. Human embryonic kidney 293 cells overexpressing OCT2 (OCT2-HEK293) and wild-type HEK293 cells (WT-HEK293) were employed. Cellular cholesterol content, assessed by thin layer chromatography, was manipulated using empty methyl- β -cyclodextrin (m β cd) and cholesterol-presaturated m β cd (RAMEB). The effect of m β cd on OCT2 protein stability and oligomerization state was evaluated by immunofluorescence and western blotting. Transport activity of OCT2 was measured using [3 H]1-methyl-4-phenylpyridinium (MPP $^+$). A 20-minute incubation with m β cd reduced total cellular cholesterol content by 40-60% as compared with that in untreated cells, without altering the content of the other main lipid species. In this condition, OCT2-mediated uptake of MPP $^+$ was reduced by ~ 50%. When cells were co-incubated with empty m β cd and cholesterol saturated m β cd (RAMEB), cholesterol content as well as OCT2-mediated uptake of MPP $^+$ were comparable to those in untreated cells, suggesting that the m β cd effect on OCT2 activity was cholesterol-dependent. In untreated cells, the MPP $^+$ influx kinetics was allosteric, whereas in cells treated with m β cd, one binding site was observed. Our findings suggest that changes in cellular cholesterol content can dramatically alter OCT2-mediated transport, potentially resulting in abnormal tubular secretion and unexpected drug toxicity and drug-drug interactions.

Significance statement

Plasma membrane cholesterol is important for the allosteric properties of OCT2. From a pharmacological standpoint, the variability in cholesterol content stemming from certain pathophysiological conditions such as aging and acute kidney injury should be taken into account as additional source of interpatient pharmacokinetics/pharmacodynamics variability and unexpected toxicity profile of OCT2 substrates, which can escape the preclinical and clinical development.

Introduction

The human organic cation transporter 2 (OCT2) is a Na⁺-independent, polyspecific cation transporter primarily located at the basolateral plasma membrane of renal proximal tubule cells. It mediates the first step of tubular secretion by translocating various substrates from the interstitium (blood side) into the proximal tubule cells. Substrates of OCT2 are several endogenous compounds, such as choline and its metabolite Trimethylamine N-oxide (TMAO), various neurotransmitters, widely used drugs like cimetidine, oxaliplatin, cisplatin, gentamicin and metformin as well as the fluorinated choline (fluorocholine), which is routinely used in positron emission tomography (PET) imaging of malignancies like brain and prostate cancer (Koepsell, 2013; Gai et al., 2016; Visentin et al., 2017; Visentin et al., 2018). The pivotal role of OCT2 in renal excretion of drugs is underscored by guidances of drug regulatory agencies, which demand that each molecule in development be tested *in vitro* for inhibition of OCT2 transport activity in order to predict potential drug-drug interactions (EMA, 2012; FDA, 2017).

As an integral membrane protein with 12 predicted transmembrane domains spanning the lipid bilayer, OCT2 is embedded in the plasma membrane, in contiguity with the variety of lipid components of the surrounding microenvironment. Especially plasma membrane cholesterol is a critical regulator of the activity of several transport proteins as well as signaling pathway receptors (Scanlon et al., 2001; Ringerike et al., 2002; Caliceti et al., 2012; Dickens et al., 2017). Firstly, by interacting with phospholipids, cholesterol regulates the fluidity of the lipid bilayer, which can dictate the mobility of the carrier and, in turn, its binding to the substrate as well as its cycling (Cooper, 1978; Chong, 1994; Radhakrishnan and McConnell, 1999; Radhakrishnan et al., 2000; Huang, 2002; Andersen and Koeppe, 2007). Additionally, cholesterol can directly interact with transmembrane proteins at the level of Cholesterol Recognition/interaction Amino acid Consensus sequences (CRAC and CARC) or areas flanking a GXXXG sequence (Fantini and Barrantes, 2013).

The plasma membrane cholesterol content of the proximal tubule cells, similar to that of other tissues, is highly dynamic and subject to substantial changes under both physiological and pathological conditions. For instance, the cholesterol-to-phospholipid ratio increases up to 25% during senescence in rat kidney membranes (Grinna, 1977; Hegner, 1980; Pratz and Corman, 1985). Additionally, mice with acute kidney injury (AKI) display a substantial (up to 50%) increase in the total membrane cholesterol level, depending on the underlying injury model (ischemia/reperfusion or obstructive nephropathy) (Zager et al., 1999). These fluctuations in membrane cholesterol content may influence the process of tubular secretion. For instance, it

has been previously shown that the transport of the organic cation tetraethylammonium (TEA) in brush-border membrane vesicles was elevated by cholesterol enrichment (Nabekura et al., 1996). The aim of the present work was to study the effect of the chemical depletion of cholesterol on OCT2 activity in intact cells overexpressing the human OCT2.

Materials and Methods

Reagents

N-Methyl-4-phenylpyridinium, acetate [N-methyl-³H]-N-Methyl-4-phenylpyridinium ([³H]MPP⁺, specific activity: 81.3 Ci/mmol) and cholesterol [4-¹⁴C]-cholesterol ([¹⁴C]cholesterol, specific activity: 50.8 mCi/mmol) were purchased from PerkinElmer (Boston, MA). Non-labeled MPP⁺, methyl- β -cyclodextrin (m β cd), cimetidine, metformin, tetraethanolamine bromide (TEA), cholesterol, sphingomyelin, phosphatidylcholine, phosphatidylserine, phosphatidylinositol and phosphatidylethanolamine were provided by Sigma-Aldrich (St.Louis, MO). Fluorocholine was purchased from BioTrend (Köln, Germany). RAMEB was provided by CycloLab Ltd. (Budapest, Hungary). Penicillin/streptomycin mixtures, Geneticin G-418 and DMEM culture medium were purchased from ThermoFisher Scientific (Waltham, MA). Biowest fetal bovine serum (FBS) was provided by VWR (Dietikon, CH). Poly-D-lysine was purchased from Corning (Bedford, MA).

Cell lines

Wild-type HEK293 cells (WT-HEK293) were maintained in Dulbecco's modified Eagle's medium (DMEM) supplemented with 10% FBS, 100 units/ml penicillin, 100 μ g/ml streptomycin at 37°C in a humidified atmosphere of 5% CO₂. Cells stably expressing the pcDNA3.1(+) plasmid containing the untagged coding sequence of the human OCT2 (OCT2-HEK293), were grown under selective pressure with Geneticin G-418 at the extracellular concentration of 400 μ g/ml (Thevenod et al., 2013).

Plasma membrane integrity assay

To assess cell membrane integrity, WT-HEK293 cells were seeded on 12-well plates coated with 0.1 mg/ml poly-D-lysine at a density of 2 x 10⁵ cells/well. After 48h cells were washed, treated for 20 minutes at 37°C with m β cd dissolved in transport buffer (116.4 mM NaCl, 5.3 mM KCl, 1 mM NaH₂PO₄, 0.8 mM MgSO₄, 5.5 mM D-glucose and 20 mM Hepes/KOH, pH 7.4), then washed with phosphate-buffered solution (PBS) and finally resuspended in a 0.02% Trypan Blue solution for cell counting.

Immunofluorescence of OCT2-HEK293 cells

Cells were seeded on chamber slides at a density of 4×10^4 cells/chamber coated with 0.1 mg/ml poly-D-lysine. Seventy-two hours later, cells were washed with cold PBS, fixed in 4% paraformaldehyde, and treated with 0.1% Triton X-100 in PBS for 15 min and with 0.1% Tween 20 in 1% BSA/PBS for 30 min. Cells were then incubated at 4 °C overnight with an antibody raised against the full-length OCT2 protein (Clone # 640438, R&D SYSTEMS, MN). After washing, the cells were mounted with DAPI (Vector Laboratories) and visualized under a fluorescent microscope (Leica DMI6000B).

Lipid extraction

Lipid extraction was performed with a standard chloroform/methanol method (Folch et al., 1951). Cells were seeded at a density of 0.5 to 1×10^6 cells/dish on 10 cm dishes pre-coated with 0.1 mg/ml poly-D-lysine. After 72 hours, cells were gently scraped from the plate and spun down for 5 minutes at $900g_{av}$. The pellet was resuspended in 1 ml of phosphate-buffered solution (PBS). One hundred μ l were lysed with 900 μ l of 0.1% (w/v) Triton X-100 in deionized water for BCA protein determination. The remaining cell suspension was mixed with 3 ml of chloroform:methanol (2:1) solution spiked with ^{14}C -cholesterol, serving as an internal standard. The amount of ^{14}C -cholesterol added as the internal standard did not exceed 1% of the total cholesterol content measured in untreated cells. After 20 min of shaking, samples were centrifuged for 5 minutes at $3000g_{av}$ for phase separation. The lower phase containing the lipid fraction was dried under a faint nitrogen flux at 30°C. Finally, the lipid pellet was resuspended in 600 μ l of ice-cold chloroform. A 50 μ l aliquot was used for assessing radioactivity by liquid scintillation counting.

Thin layer chromatography (TLC)

For analysis of the cholesterol and phospholipid content, aliquots from the extracted lipids were loaded on HPTLC Silica gel 60 plates with a concentrating zone (Merck KGaA, Darmstadt, Germany) using an automated Camag TLC sampler ATS4 and separated by one-dimensional thin layer chromatography (TLC). Cholesterol was resolved in 62.3% n-hexane, 18.3% n-heptane, 18.4% diethyl ether and 1% acetic acid. Phospholipids were resolved in 26.6% Methyl acetate (v/v), 26.6% 1-propanol (v/v), 26.6% chloroform (v/v), 10.6% methanol (v/v) and 0.05% KCl (w/v). Staining was performed in 9.6% ortho phosphoric acid (v/v) and 3% copper acetate (w/v), and then the plate was dried at 120°C for 30 minutes. Bands were scanned at 366

nm and absolute quantification performed from a serial dilution of the main lipid species separated in parallel. The values were then normalized for the [^{14}C]cholesterol recovery yield and the protein content.

Cell surface labelling

Nearly confluent OCT2-HEK293 cells were washed twice with PBS and treated with 1 mg/ml EZ-Link Sulfo-NHS-LC-biotin in PBS on ice for 1 hour. This non-permeable reagent alkylates accessible Lys residues. Cells were then washed twice and incubated for 30 minutes with hypotonic buffer (0.5 mM Na_2HPO_4 and 0.1 mM EDTA at pH 7.0) containing protease inhibitors. Cells were then scraped from the plates and centrifuged at $16000g_{\text{av}}$ for 15 minutes at 4°C . The pellet was lysed in 200 μl of lysis buffer (0.1% SDS, 1% Triton X-100, 1 mM EDTA, 150 mM NaCl, and 20 mM Tris, pH 7.4) containing protease inhibitors and rotated for 2 hours at 4°C , then spun down at $16,000g_{\text{av}}$ at 4°C for 15 minutes. A portion of the supernatant was used for BCA protein determination and for total lysate analysis. The remaining portion was mixed with streptavidin-agarose beads (50 μl /sample) overnight at 4°C . The beads were washed twice in lysis buffer and twice in lysis buffer supplemented with 2% (w/v) SDS. After the final wash, bead-bound proteins were stripped, incubating the samples at 95°C for 5 minutes in Laemmli buffer containing 1.5% (w/v) dithiothreitol (DTT) and loaded directly onto polyacrylamide gels. Total lysate samples were denatured using the same conditions.

SDS Gel Electrophoresis and Western Blotting

Surface labelling protein samples and the respective total lysates were resolved on 8% (w/v) polyacrylamide gels. To assess the OCT2 oligomerization state, total lysate samples were denatured for 15 minutes at 50°C in Laemmli buffer with or without 1.5% DTT (w/v), then resolved on a gel with a 6-12% (w/v) gradient of polyacrylamide. Proteins were electroblotted onto nitrocellulose membranes (GE HealthCare, Piscataway, NJ). The membranes were blocked with 5% (w/v) non-fat dry milk in PBS supplemented with 0.1% (w/v) Tween 20 (PBS-T) and incubated overnight at 4°C with anti-OCT2 (Clone # 640438, R&D SYSTEMS, MN), followed by probing with a horseradish peroxidase-conjugated secondary antibody. Blots were developed with SuperSignal West Femto Maximum Sensitivity Substrate (Thermo Scientific, Waltham, MA) and Fusion FX7 (Vilber Lourmat, Eberhardzell, Germany). As a control, the sample blots were probed with anti-pan-actin.

Transport Studies in Intact Cells

Uptake of radiolabeled compounds was measured using a protocol designed for uptake determination in cells (Schroeder et al., 1998; Visentin et al., 2015). WT-HEK293 and OCT2-HEK293 cells were seeded at a density of 2.5×10^5 cells/dish on 35-mm dishes coated with 0.1 mg/ml poly-D-lysine (Corning, Bedford, MA). After 72 hours, cells were washed and equilibrated in transport buffer (116.4 mM NaCl, 5.3 mM KCl, 1 mM NaH_2PO_4 , 0.8 mM MgSO_4 , 5.5 mM D-glucose and 20 mM Hepes/KOH, pH 7.4) at 37°C, then the buffer was aspirated and transport buffer containing the radiolabelled substrate was added. Uptake was stopped by quick aspiration followed by extensive washing with ice-cold transport buffer. Cells were solubilized and intracellular radioactivity was assessed by liquid scintillation counting. Protein content was determined by the bicinchoninic acid protein assay (Interchim, Montluçon Cedex, France). OCT2-independent uptake was determined in WT-HEK293 cells and subtracted from the total uptake to quantify the OCT2-mediated transport. Uptake is expressed as picomoles of substrate per milligram of protein.

Statistical Analysis

Statistical comparisons were performed using GraphPad Prism (version 5.0 for Windows, GraphPad Software). Comparisons between two groups were performed with the two-tailed Student's unpaired t-test. For multiple comparisons, one-way analysis of variance (one-way ANOVA) followed by Bonferroni's post-hoc test was employed.

Results

Acute exposure to m β cd removed cholesterol without changing the content of the other major classes of lipids nor affecting cell membrane integrity

Cyclodextrins are torus-shaped cyclic oligosaccharides with a hydrophobic inner cavity that attracts and encapsulates non-polar substances in close proximity. Among cyclodextrin molecules, methyl- β -cyclodextrin (m β cd) preferentially accepts and scavenges cholesterol (Zidovetzki and Levitan, 2007). WT-HEK293 cells exposed to m β cd for 20 minutes showed a dose-dependent cholesterol depletion (Figure 1A). At the highest extracellular concentration of m β cd tested, the total cholesterol content of WT- and OCT2-HEK293 cells was reduced by ~60% and 40% respectively, as compared with the respective untreated cells (Figure 1B). Because most of the cellular cholesterol resides within the plasma membrane, it can be assumed that total cholesterol content reflects that of the plasma membrane (Lange et al., 1989). Because cholesterol has a time- and concentration-dependent effect on membrane organization and permeability (Raffy and Teissie, 1999), the effect of m β cd-induced cholesterol depletion on membrane permeability was also assessed. WT- and OCT2-HEK293 cells were exposed for 20 minutes to increasing extracellular concentrations of m β cd and then mixed with Trypan blue solution for cell counting. Figure 1C shows that the majority of cells were impermeable to Trypan blue, suggesting preserved membrane integrity. While m β cd is considered relatively specific for cholesterol, some studies have reported the depletion of other lipids as well (Ottico et al., 2003; Giocondi et al., 2004; Monnaert et al., 2004). After a 20-minute incubation of WT- and OCT2-HEK293 cells with m β cd at an extracellular concentration of 10 mM, no obvious depletion of the other major classes of lipids was observed (Figure 2A-F).

M β cd exposure impaired MPP⁺ influx mediated by OCT2

Figure 3A illustrates the time course of MPP⁺ uptake over 15 minutes at an extracellular concentration of 0.5 μ M at pH 7.4 in WT- and OCT2-HEK293 cells. The increase in intracellular MPP⁺ rapidly deviated from linearity, reaching the equilibrium within 5 minutes. The time course over a shorter interval showed that MPP⁺ uptake as a function of time was linear over 15 seconds, reflecting the unidirectional flux of MPP⁺ into the cells. The transport rate of MPP⁺ in OCT2-HEK293 cells was ~36 times higher than that in the WT-HEK293 cells (slope, 0.36 ± 0.01 vs 0.01 ± 0.02 pmol mg⁻¹ s⁻¹) (Fig. 3B). Based on the time course, the effect of a 20-minute pre-incubation with m β cd on OCT2-mediated MPP⁺ transport was assessed over

a 5-second interval at an MPP^+ extracellular concentration of $0.5 \mu\text{M}$. In figure 3C, it can be seen that MPP^+ influx was significantly lower in the $\text{m}\beta\text{cd}$ -treated cells in comparison with that in the untreated cells (36.4 ± 5.9 vs $22.2 \pm 3.3 \text{ pmol mg}^{-1} \text{ min}^{-1}$). To rule out any direct effect of $\text{m}\beta\text{cd}$ on OCT2, a *cis*-inhibition assay was performed. Figure 3D shows that $\text{m}\beta\text{cd}$ co-incubation had no effect on MPP^+ OCT2-mediated influx (100.0 ± 14.9 vs $110.8 \pm 36.9 \text{ pmol mg}^{-1} \text{ min}^{-1}$). For the *cis*-inhibition control, cells were exposed to non-labelled MPP^+ at an extracellular concentration of 1 mM .

Incubation with $\text{m}\beta\text{cd}$ -RAMEB mixture did not alter total cholesterol levels and OCT2-mediated MPP^+ influx

$\text{M}\beta\text{cd}$ may have multiple non-specific effects in addition to cholesterol depletion (Ormerod et al., 2012). To assess whether the effect of $\text{m}\beta\text{cd}$ on OCT2-mediated MPP^+ influx was indeed the result of cholesterol depletion, “cholesterol-matched” experiments were performed. To determine the cholesterol equilibrium point, different ratios of empty $\text{m}\beta\text{cd}$ and RAMEB (cholesterol-saturated $\text{m}\beta\text{cd}$) were tested in WT- and OCT2-HEK293 cells. It can be seen that cells exposed for 20 minutes to a 1:1 $\text{m}\beta\text{cd}$:RAMEB mixture showed similar total cholesterol content to that of control cells (Figure 4A and B). Figure 4C shows that the MPP^+ influx mediated by OCT2 in cells exposed to 1:1 $\text{m}\beta\text{cd}$:RAMEB was comparable to that in control cells, suggesting that the transport of MPP^+ was reduced only when membrane cholesterol was depleted.

$\text{M}\beta\text{cd}$ did not alter cell surface expression of OCT2

The impact of cellular cholesterol manipulation on OCT2 protein level and localization was assessed by western blotting of the plasma membrane OCT2, pulled down by lysine residue labelling (Figure 5A) and by immunofluorescence and (Figure 5B). It can be seen that the treatment with $\text{m}\beta\text{cd}$ at an extracellular concentration of 10 mM did not appear to affect the surface expression of OCT2. The selective labelling of the plasma membrane protein fraction was confirmed by the negative probing for actin (Figure 5A).

$\text{M}\beta\text{cd}$ exposure did not affect OCT2 oligomerization state

It has previously been shown that OCT2 exists in monomeric and oligomeric states and that disruption of oligomerization by DTT exposure or mutagenesis of specific cysteine residues reduced OCT2 transport rate (Brast et al., 2012). The oligomerization state of OCT2 after mβcd treatment was assessed by western blotting under non-reducing conditions. In figure 5C it can be seen that most OCT2 appears to be in the monomer state and a weaker band is observed at the size compatible with a tetramer, although the presence of heterocomplex cannot be excluded. No obvious change that can explain the dramatic effect of mβcd on OCT2-mediated MPP⁺ influx kinetics can be appreciated.

Incubation with mβcd shifted OCT2-mediated MPP[±] influx kinetics from sigmoidal to hyperbolic

The kinetic basis underlying the reduced MPP⁺ influx upon cholesterol removal was assessed by measuring the OCT2-mediated influx (5 seconds) of MPP⁺ as a function of the extracellular concentration of substrate after a 20-minute preincubation with mβcd at an extracellular concentration of 10 mM. Figure 6A to C show a sigmoidal and a hyperbolic curve of MPP⁺ OCT2-mediated influx in control and mβcd-treated cells, respectively, suggesting that the removal of cholesterol abolished the allosteric binding of MPP⁺ to OCT2. The switch from homotropic positive cooperativity to one-binding site kinetics was confirmed by the Eadie-Hofstee and Hill linear transformations (Figure 6D-F and Table 1).

Discussion

OCT2-mediated influx kinetics that deviate from the classic hyperbole (one binding site kinetics) to the sigmoid with two cooperative binding sites is not surprising and was previously shown for gentamicin and choline by our group (Gai et al., 2016; Visentin et al., 2018). Moreover, the presence of multiple interacting binding sites has been described studying the rat OCT1, whose protein sequence is 69% identical to that of the human OCT2 (Gorbunov et al., 2008; Minuesa et al., 2009; Minuesa et al., 2017). Nonetheless, for the very same substrates, one binding site kinetics for the human OCT2 have been reported as well. These discordant results may stem from the varying *in vitro* models used in these studies: OCT2-mediated influx has been described as the classic hyperbola consistent with the Michaelis-Menten model in *Xenopus laevis* oocytes and in CHO cells, and as sigmoid in HEK293 cells (Gorboulev et al., 1997; Budiman et al., 2000; Gai et al., 2016; Severance et al., 2017; Visentin et al., 2018). Here we show that after cholesterol depletion by exposure to the oligosaccharide m β cd, MPP⁺ uptake in HEK293 cells overexpressing OCT2 loses the allosterism and best fits the Michaelis-Menten equation. Noteworthy, the MPP⁺ influx kinetics in OCT2-HEK293 cells depleted of cholesterol reconciles with previously published data using alternative models, with a calculated OCT2-mediated MPP⁺ influx K_m (Table 1) comparable to those computed from uptake values measured in *Xenopus laevis* oocytes (1.2 μ M) or in Chinese Hamster Ovary (CHO) cells overexpressing OCT2 (3.9 μ M) (Gorboulev et al., 1997; Severance et al., 2017). In order to clarify the contribution of cholesterol content on the discrepancies observed among experimental models, it will be interesting to perform head-to-head assessment of lipid content and influx kinetics in the different models. Cholesterol-dependent allosterism has previously been reported for other transmembrane proteins, including Mg⁺⁺- and Na⁺/K⁺-ATPase, acetylcholinesterase and the transport of estradiol-17- β -glucuronide (E17 β G) by the multidrug resistance-associated protein 2 (MRP2) (Bloj et al., 1973a; Bloj et al., 1973b; Guyot et al., 2014). Notably, cholesterol can either promote or inhibit allosterism and the effect seems to be enzyme-dependent. While cholesterol induced allosterism of OCT2 as well as of Mg⁺⁺- and Na⁺/K⁺-ATPase, MRP2 and acetylcholinesterase allosteric binding was observed only in the absence of cholesterol (Bloj et al., 1973a; Guyot et al., 2014).

OCT2 has been shown to exist at the plasma membrane in monomeric and oligomeric form (Brast et al., 2012). Oligomerization is an important determinant of correct localization, function and regulation of different transporter proteins and membrane lipid composition can affect the oligomerization state of the transmembrane proteins embedded therein (Mors et al., 2013; Alguel et al., 2016; Gupta et al., 2017). Because the removal of cholesterol from OCT2-

HEK293 cells did not seem to alter the equilibria between the different states of oligomerization observed for this transporter, it is plausible to hypothesize that the allostereism is a feature of OCT2 binding pockets regardless of the oligomerization state. In line with this, Keller and colleagues recently showed that cell-free-expressed rat OCT1 reconstituted in nanodiscs or proteoliposomes displayed one high-affinity binding site and two low-affinity binding sites for MPP⁺ per transporter monomer, with the latter two being responsible for the transport and the first one serving exclusively as an allosteric site (Keller et al., 2019). Interestingly, when the binding of the rat OCT1 monomer was assessed in nanodiscs formed with 1,2-dimyristoyl-*sn*-glycero-3-phospho-(1-*rac*-glycerol) (DMPG) or 1-palmitoyl-2-oleoyl-*sn*-glycero-3-phosphocholine (POPC) and 1,2-dipalmitoyl-*sn*-glycero-3-phosphocholine (DPPC), only two low-affinity binding sites with overlapping K_D were detected with the high affinity binding site not being accessible. However, when the binding was assessed in the presence of 1,2-diacyl-*sn*-glycerol—phospho-L-serine, 1,2-diacyl-*sn*-glycero-3-phosphocholine and cholesterol, three binding sites were detected with three calculated K_D values: 0.1, 10 and 36 μ M, indicating that the lipid composition regulates rat OCT1 allosteric binding (Keller et al., 2019). It is possible that the human OCT2 is equipped with a high-affinity binding site that regulates the allostereism between two low-affinity binding sites as well. However, this needs to be addressed using similar synthetic approaches.

Multispecificity and allostereism are pillars of efficient detoxifying proteins including transporters (Bodo et al., 2003; Zelcer et al., 2003; Hirono et al., 2005). While multispecificity allows recognizing a broad range of molecules, allostereism confers the ability to adapt to increasing concentrations of substrates. This is evident in figure 5: the loss of allostereism upon cholesterol depletion led to a rapid saturation of the OCT2 transport molecules and, in turn, to a limited transport capacity. Because OCT2 plays a key role in the clearance of many drugs and toxins, it is conceivable that pathophysiological changes in renal membrane cholesterol content may shift the OCT2 kinetics from hyperbolic to sigmoidal, or vice versa. Moreover, upon cholesterol depletion, the inhibitory effect of certain OCT2 substrates on MPP⁺ uptake was reduced, whereas for some others it was enhanced in comparison to that in the presence of cholesterol, indicating that changes in the cholesterol content alter, to some extent, the substrate specificity of the carrier.

It has been previously shown that OCT2 expression varies in several pathophysiological conditions. Rats with acute kidney injury showed lower Oct2 levels (Ji et al., 2002; Matsuzaki et al., 2008; Shim et al., 2009; Maeng et al., 2012). Obesity, both in human and in mice, induces

OCT2 expression (Gai et al., 2016). Renal cell carcinoma cells have low OCT2 levels as compared with the surrounding normal tissue (Liu et al., 2016; Visentin et al., 2018). This work adds another level of complexity in the study of OCT2-mediated tubular secretion in renal pathology.

Acknowledgments

The authors would like to thank Hermann Koepsell, University of Wurzburg, for providing OCT2-HEK293 cells.

Authorship contributions

Participated in research design: Hörmann, Kullak-Ublick, Visentin.

Conducted experiments: Hörmann, Gai, Visentin.

Performed data analysis: Hörmann, Visentin.

Contribution to manuscript writing: Hörmann, Visentin.

Approval of the final manuscript: Hörmann, Gai, Kullak-Ublick, Visentin.

References

- Alguel Y, Cameron AD, Diallinas G and Byrne B (2016) Transporter oligomerization: form and function. *Biochemical Society transactions* **44**:1737-1744.
- Andersen OS and Koeppe RE, 2nd (2007) Bilayer thickness and membrane protein function: an energetic perspective. *Annu Rev Biophys Biomol Struct* **36**:107-130.
- Bloj B, Morero RD and Farias RN (1973a) Membrane fluidity, cholesterol and allosteric transitions of membrane-bound Mg^{2+} -ATPase, $(Na^{+} + K^{+})$ -ATPase and acetylcholinesterase from rat erythrocytes. *FEBS letters* **38**:101-105.
- Bloj B, Morero RD, Farias RN and Trucco RE (1973b) Membrane lipid fatty acids and regulation of membrane-bound enzymes. Allosteric behaviour of erythrocyte Mg^{2+} -ATPase, $(Na^{+} + K^{+})$ -ATPase and acetylcholinesterase from rats fed different fat-supplemented diets. *Biochimica et biophysica acta* **311**:67-79.
- Bodo A, Bakos E, Szeri F, Varadi A and Sarkadi B (2003) Differential modulation of the human liver conjugate transporters MRP2 and MRP3 by bile acids and organic anions. *The Journal of biological chemistry* **278**:23529-23537.
- Brast S, Grabner A, Sucic S, Sitte HH, Hermann E, Pavenstadt H, Schlatter E and Ciarimboli G (2012) The cysteines of the extracellular loop are crucial for trafficking of human organic cation transporter 2 to the plasma membrane and are involved in oligomerization. *FASEB journal : official publication of the Federation of American Societies for Experimental Biology* **26**:976-986.
- Budiman T, Bamberg E, Koepsell H and Nagel G (2000) Mechanism of electrogenic cation transport by the cloned organic cation transporter 2 from rat. *The Journal of biological chemistry* **275**:29413-29420.
- Caliceti C, Zambonin L, Prata C, Vieceli Dalla Sega F, Hakim G, Hrelia S and Fiorentini D (2012) Effect of plasma membrane cholesterol depletion on glucose transport regulation in leukemia cells. *PloS one* **7**:e41246.
- Chong PL (1994) Evidence for regular distribution of sterols in liquid crystalline phosphatidylcholine bilayers. *Proceedings of the National Academy of Sciences of the United States of America* **91**:10069-10073.
- Cooper RA (1978) Influence of increased membrane cholesterol on membrane fluidity and cell function in human red blood cells. *J Supramol Struct* **8**:413-430.
- Dickens D, Chiduzza GN, Wright GS, Pirmohamed M, Antonyuk SV and Hasnain SS (2017) Modulation of LAT1 (SLC7A5) transporter activity and stability by membrane cholesterol. *Sci Rep* **7**:43580.

- EMA (2012) Guideline on the investigation of drug interactions, in, http://www.ema.europa.eu/docs/en_GB/document_library/Scientific_guideline/2012/07/WC500129606.pdf.
- Fantini J and Barrantes FJ (2013) How cholesterol interacts with membrane proteins: an exploration of cholesterol-binding sites including CRAC, CARC, and tilted domains. *Front Physiol* **4**:31.
- FDA U (2017) In Vitro Metabolism- and Transporter- Mediated Drug-Drug Interaction Studies Guidance for Industry, in, <http://www.fda.gov/Drugs/GuidanceComplianceRegulatoryInformation/Guidances/default.htm>.
- Folch J, Ascoli I, Lees M, Meath JA and Le BN (1951) Preparation of lipide extracts from brain tissue. *The Journal of biological chemistry* **191**:833-841.
- Gai Z, Visentin M, Hiller C, Krajnc E, Li T, Zhen J and Kullak-Ublick GA (2016) Organic Cation Transporter 2 (OCT2-SLC22A2) overexpression may confer an increased risk of gentamicin-induced nephrotoxicity. *Antimicrobial agents and chemotherapy*.
- Giocondi MC, Milhiet PE, Dosset P and Le Grimellec C (2004) Use of cyclodextrin for AFM monitoring of model raft formation. *Biophysical journal* **86**:861-869.
- Gorboulev V, Ulzheimer JC, Akhoundova A, Ulzheimer-Teuber I, Karbach U, Quester S, Baumann C, Lang F, Busch AE and Koepsell H (1997) Cloning and characterization of two human polyspecific organic cation transporters. *DNA and cell biology* **16**:871-881.
- Gorbunov D, Gorboulev V, Shatskaya N, Mueller T, Bamberg E, Friedrich T and Koepsell H (2008) High-affinity cation binding to organic cation transporter 1 induces movement of helix 11 and blocks transport after mutations in a modeled interaction domain between two helices. *Molecular pharmacology* **73**:50-61.
- Grinna LS (1977) Age related changes in the lipids of the microsomal and the mitochondrial membranes of rat liver and kidney. *Mech Ageing Dev* **6**:197-205.
- Gupta K, Donlan JAC, Hopper JTS, Uzdavinys P, Landreh M, Struwe WB, Drew D, Baldwin AJ, Stansfeld PJ and Robinson CV (2017) The role of interfacial lipids in stabilizing membrane protein oligomers. *Nature* **541**:421-424.
- Guyot C, Hofstetter L and Stieger B (2014) Differential effects of membrane cholesterol content on the transport activity of multidrug resistance-associated protein 2 (ABCC2) and of the bile salt export pump (ABCB11). *Molecular pharmacology* **85**:909-920.
- Hegner D (1980) Age-dependence of molecular and functional changes in biological membrane properties. *Mech Ageing Dev* **14**:101-118.

- Hirono S, Nakagome I, Imai R, Maeda K, Kusuhara H and Sugiyama Y (2005) Estimation of the three-dimensional pharmacophore of ligands for rat multidrug-resistance-associated protein 2 using ligand-based drug design techniques. *Pharmaceutical research* **22**:260-269.
- Huang J (2002) Exploration of molecular interactions in cholesterol superlattices: effect of multibody interactions. *Biophysical journal* **83**:1014-1025.
- Ji L, Masuda S, Saito H and Inui K (2002) Down-regulation of rat organic cation transporter rOCT2 by 5/6 nephrectomy. *Kidney international* **62**:514-524.
- Keller T, Gorboulev V, Mueller TD, Dotsch V, Bernhard F and Koepsell H (2019) Rat Organic Cation Transporter 1 Contains Three Binding Sites for Substrate 1-Methyl-4-phenylpyridinium per Monomer. *Molecular pharmacology* **95**:169-182.
- Koepsell H (2013) The SLC22 family with transporters of organic cations, anions and zwitterions. *Molecular aspects of medicine* **34**:413-435.
- Lange Y, Swaisgood MH, Ramos BV and Steck TL (1989) Plasma membranes contain half the phospholipid and 90% of the cholesterol and sphingomyelin in cultured human fibroblasts. *The Journal of biological chemistry* **264**:3786-3793.
- Liu Y, Zheng X, Yu Q, Wang H, Tan F, Zhu Q, Yuan L, Jiang H, Yu L and Zeng S (2016) Epigenetic activation of the drug transporter OCT2 sensitizes renal cell carcinoma to oxaliplatin. *Sci Transl Med* **8**:348ra397.
- Maeng HJ, Shim WS, Ahn SJ, Yu SS, Kim DD, Shim CK and Chung SJ (2012) Differential changes in functional activity of organic cation transporters in rats with uranyl nitrate-induced acute renal failure. *Archives of pharmacal research* **35**:1441-1448.
- Matsuzaki T, Morisaki T, Sugimoto W, Yokoo K, Sato D, Nonoguchi H, Tomita K, Terada T, Inui K, Hamada A and Saito H (2008) Altered pharmacokinetics of cationic drugs caused by down-regulation of renal rat organic cation transporter 2 (Slc22a2) and rat multidrug and toxin extrusion 1 (Slc47a1) in ischemia/reperfusion-induced acute kidney injury. *Drug metabolism and disposition: the biological fate of chemicals* **36**:649-654.
- Minuesa G, Albert C, Pastor-Anglada M, Martinez-Picado J and Koepsell H (2017) Response to "Tenofovir Disoproxil Fumarate Is Not an Inhibitor of Human Organic Cation Transporter 1". *The Journal of pharmacology and experimental therapeutics* **360**:343-345.
- Minuesa G, Volk C, Molina-Arcas M, Gorboulev V, Erkizia I, Arndt P, Clotet B, Pastor-Anglada M, Koepsell H and Martinez-Picado J (2009) Transport of lamivudine [(-)-beta-L-2',3'-dideoxy-3'-thiacytidine] and high-affinity interaction of nucleoside reverse

- transcriptase inhibitors with human organic cation transporters 1, 2, and 3. *The Journal of pharmacology and experimental therapeutics* **329**:252-261.
- Monnaert V, Tilloy S, Bricout H, Fenart L, Cecchelli R and Monflier E (2004) Behavior of alpha-, beta-, and gamma-cyclodextrins and their derivatives on an in vitro model of blood-brain barrier. *The Journal of pharmacology and experimental therapeutics* **310**:745-751.
- Mors K, Hellmich UA, Basting D, Marchand P, Wurm JP, Haase W and Glaubitz C (2013) A lipid-dependent link between activity and oligomerization state of the M. tuberculosis SMR protein TBsmr. *Biochimica et biophysica acta* **1828**:561-567.
- Nabekura T, Takano M and Inui K (1996) Cholesterol modulates organic cation transport activity and lipid fluidity in rat renal brush-border membranes. *Biochimica et biophysica acta* **1283**:232-236.
- Ormerod KG, Rogasevskaia TP, Coorssen JR and Mercier AJ (2012) Cholesterol-independent effects of methyl-beta-cyclodextrin on chemical synapses. *PloS one* **7**:e36395.
- Ottico E, Prinetti A, Prioni S, Giannotta C, Basso L, Chigorno V and Sonnino S (2003) Dynamics of membrane lipid domains in neuronal cells differentiated in culture. *Journal of lipid research* **44**:2142-2151.
- Pratz J and Corman B (1985) Age-related changes in enzyme activities, protein content and lipid composition of rat kidney brush-border membrane. *Biochimica et biophysica acta* **814**:265-273.
- Radhakrishnan A, Anderson TG and McConnell HM (2000) Condensed complexes, rafts, and the chemical activity of cholesterol in membranes. *Proceedings of the National Academy of Sciences of the United States of America* **97**:12422-12427.
- Radhakrishnan A and McConnell HM (1999) Condensed complexes of cholesterol and phospholipids. *Biophysical journal* **77**:1507-1517.
- Raffy S and Teissie J (1999) Control of lipid membrane stability by cholesterol content. *Biophysical journal* **76**:2072-2080.
- Ringerike T, Blystad FD, Levy FO, Madhus IH and Stang E (2002) Cholesterol is important in control of EGF receptor kinase activity but EGF receptors are not concentrated in caveolae. *Journal of cell science* **115**:1331-1340.
- Scanlon SM, Williams DC and Schloss P (2001) Membrane cholesterol modulates serotonin transporter activity. *Biochemistry* **40**:10507-10513.
- Schroeder A, Eckhardt U, Stieger B, Tynes R, Schteingart CD, Hofmann AF, Meier PJ and Hagenbuch B (1998) Substrate specificity of the rat liver Na(+)-bile salt cotransporter

- in *Xenopus laevis* oocytes and in CHO cells. *The American journal of physiology* **274**:G370-375.
- Severance AC, Sandoval PJ and Wright SH (2017) Correlation between Apparent Substrate Affinity and OCT2 Transport Turnover. *The Journal of pharmacology and experimental therapeutics* **362**:405-412.
- Shim WS, Park JH, Ahn SJ, Han L, Jin QR, Li H, Choi MK, Kim DD, Chung SJ and Shim CK (2009) Testosterone-independent down-regulation of Oct2 in the kidney medulla from a uranyl nitrate-induced rat model of acute renal failure: effects on distribution of a model organic cation, tetraethylammonium. *Journal of pharmaceutical sciences* **98**:739-747.
- Thevenod F, Ciarimboli G, Leistner M, Wolff NA, Lee WK, Schatz I, Keller T, Al-Monajjed R, Gorboulev V and Koepsell H (2013) Substrate- and cell contact-dependent inhibitor affinity of human organic cation transporter 2: studies with two classical organic cation substrates and the novel substrate cd2+. *Molecular pharmaceutics* **10**:3045-3056.
- Visentin M, Stieger B, Merz M and Kullak-Ublick GA (2015) Octreotide Inhibits the Bilirubin Carriers Organic Anion Transporting Polypeptides 1B1 and 1B3 and the Multidrug Resistance-Associated Protein 2. *The Journal of pharmacology and experimental therapeutics* **355**:145-151.
- Visentin M, Torozi A, Gai Z, Hausler S, Li C, Hiller C, Schraml PH, Moch H and Kullak-Ublick GA (2018) Fluorocholine Transport Mediated by the Organic Cation Transporter 2 (OCT2, SLC22A2): Implication for Imaging of Kidney Tumors. *Drug metabolism and disposition: the biological fate of chemicals* **46**:1129-1136.
- Visentin M, van Rosmalen BV, Hiller C, Bieze M, Hofstetter L, Verheij J, Kullak-Ublick GA, Koepsell H, Phoa SS, Tamai I, Bennis RJ, van Gulik TM and Stieger B (2017) Impact of Organic Cation Transporters (OCT-SLC22A) on Differential Diagnosis of Intrahepatic Lesions. *Drug metabolism and disposition: the biological fate of chemicals* **45**:166-173.
- Zager RA, Burkhart KM, Johnson AC and Sacks BM (1999) Increased proximal tubular cholesterol content: implications for cell injury and "acquired cytoresistance". *Kidney international* **56**:1788-1797.
- Zelcer N, Huisman MT, Reid G, Wielinga P, Breedveld P, Kuil A, Knipscheer P, Schellens JH, Schinkel AH and Borst P (2003) Evidence for two interacting ligand binding sites in human multidrug resistance protein 2 (ATP binding cassette C2). *The Journal of biological chemistry* **278**:23538-23544.

Zidovetzki R and Levitan I (2007) Use of cyclodextrins to manipulate plasma membrane cholesterol content: evidence, misconceptions and control strategies. *Biochimica et biophysica acta* **1768**:1311-1324.

Footnotes

This work was supported by the Swiss National Science Foundation to GAK-U [310030_175639].

Legends for Figures

Figure 1. Cholesterol content and membrane integrity of WT- and OCT2-HEK293 upon 20-minute incubation with mβcd. Representative TLC plate from WT-HEK293 cells (A). Quantification of total cholesterol. Data are relative to the cholesterol content in untreated cells (B). Percentage of cells impermeable to Trypan Blue dye (C). All results represent the mean ± S.D. from three independent experiments.

Figure 2. Phospholipid content of WT- and OCT2-HEK293 upon 20-minute incubation with mβcd. Representative TLC plate of the main lipid species from WT-HEK293 cells (A). Quantification of total sphingomyelin (SM), phosphatidylcholine (PC), phosphatidylserine (PS), phosphatidylinositol (PI) and phosphatidylethanolamine (PE) content. Data are relative to the respective content in untreated cells and represent the mean ± S.D from three independent experiments (B-F).

Figure 3. OCT2-mediated MPP⁺ transport. Time course of MPP⁺ at the extracellular concentrations of 0.5 μM in WT- and OCT2-HEK293 cells. Representative of two independent experiments (A-B). OCT2-mediated MPP⁺ influx at the extracellular concentrations of 0.5 μM after 20-minute incubation with mβcd. Data were corrected for uptake in WT-HEK293 cells and represent the mean ± S.D. from three independent experiments (C). OCT2-mediated MPP⁺ influx rate at the extracellular concentration of 1 μM in the presence of mβcd. Co-incubation with non-labelled MPP⁺ was used as positive control. Uptake values in WT-HEK293 were subtracted and results expressed as the mean ± S.D. from three independent experiments (D).

Figure 4. Cholesterol content and OCT2-mediated MPP⁺ influx after 20-minute exposure to mβcd-RAMEB mixtures. Representative TLC plate of the cholesterol content in WT-HEK293 cells after incubation with the indicated ratios of mβcd and RAMEB (mβcd containing cholesterol) (A). Cholesterol content quantification. Data are relative to the cholesterol content in untreated cells and represent the mean ± S.D from three independent experiments (B). Uptake of MPP⁺ (1 μM) after 20-minute incubation with mβcd or 1:1 mβcd:RAMEB. Data were corrected for uptake in WT-HEK293 cells and represent the mean ± S.D. from two independent experiments performed in duplicate (C).

Figure 5. Western blotting and immunofluorescence of OCT2. Representative Western blots from three independent experiments of OCT2 expression biotinylated at the cell surface (1, 2 and 3) and in the total lysate (4, 5 and 6); actin and Na⁺/K⁺ controls are shown. Lanes 1 and 4 are loaded with samples from control OCT2-HEK293 cells, lanes 2 and 5 with samples

from OCT2-HEK293 cells exposed to 10 mM mβcd for 20 minutes. Samples from OCT2-HEK293 cells incubated without biotinylation reagent are shown in lanes 3 and 6 (A). Representative Immunostaining from three independent experiments of OCT2 after 20-minute incubation with mβcd. Scale bar = 100 μm (B). Representative Western blot of cell lysates from OCT2-HEK293 treated for 20 minutes with or without mβcd and then denaturated in the presence or absence of DTT. The experiment was performed three times (C).

Figure 6. Kinetic analysis of MPP⁺ influx. Initial uptake of increasing extracellular concentrations of MPP⁺ was assessed over 5 seconds in OCT2-HEK293 cells after 20-minute incubation with mβcd. All data were corrected for uptake in WT-HEK293 cells. Line was best fit to an allosteric sigmoidal equation $Y = V_{\max} * X^h / (K_{\text{prime}} + X^h)$, where K_{prime} is an estimation of K_m , V_{\max} is the maximum capacity and h is the Hill slope (A). Enlargement of the first part of OCT2 influx kinetics in control- (B) and mβcd-treated (C) cells. Eadie-Hofstee transformation in control (D) and mβcd-treated cells (E). Hill transformation (F). Results represent the mean ± S.D. from four independent experiments.

Tables

Table 1. Kinetic parameters of MPP⁺ influx mediated by OCT2 after mβcd treatment.

Analysis	K _m (μM) (mean ± SD)	V _{max} (pmol mg ⁻¹ min ⁻¹) (mean ± SD)	Hill slope (mean ± SD)
Control			
Nonlinear regression	46.7±32.5	2611±216	1.61±0.34
Eadie-Hofstee	-	-	-
Hill	-	-	1.50±0.11
mβcd			
Nonlinear regression	4.75 ± 2.44	624 ± 88.3	1.03 ± 0.41
Eadie-Hofstee	4.77 ± 0.78	632 ± 43.7	-
Hill	-	-	0.98 ± 0.05

Figure 1

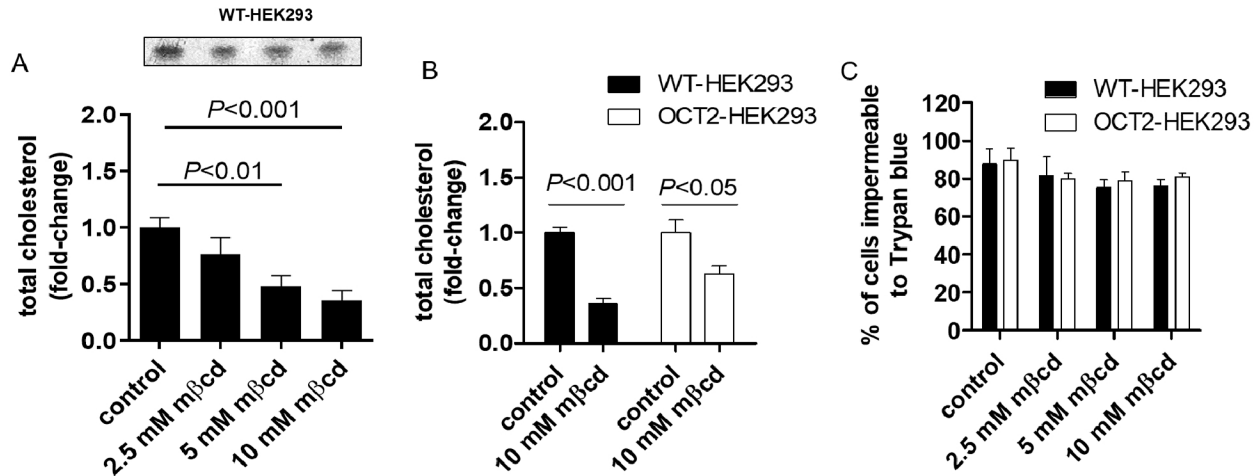


Figure 2

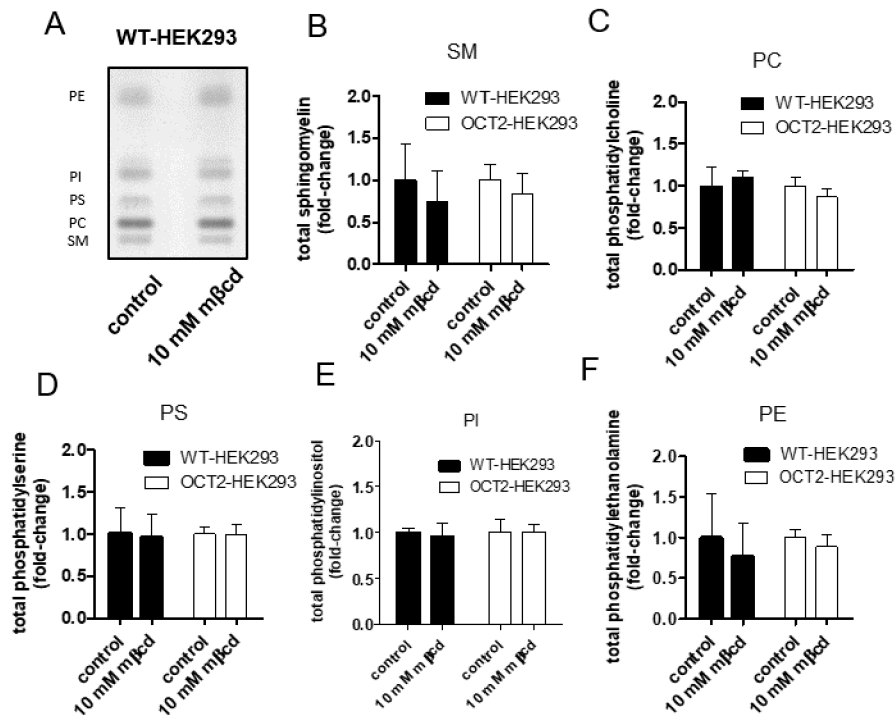


Figure 3

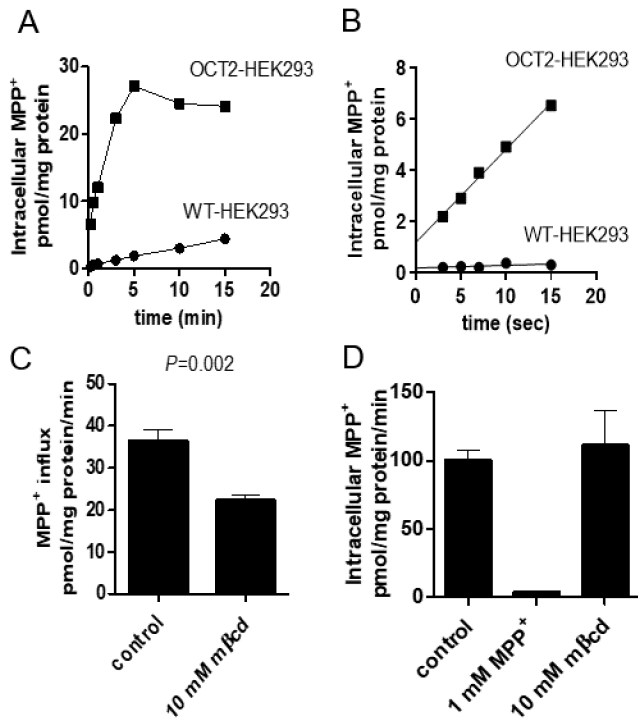
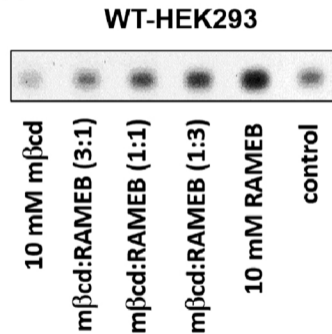
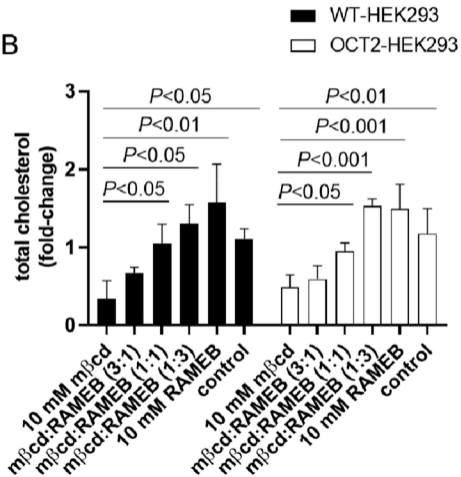


Figure 4

A



B



C

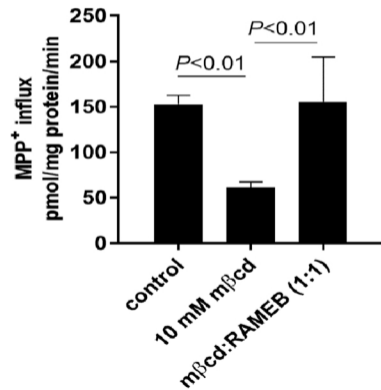


Figure 5

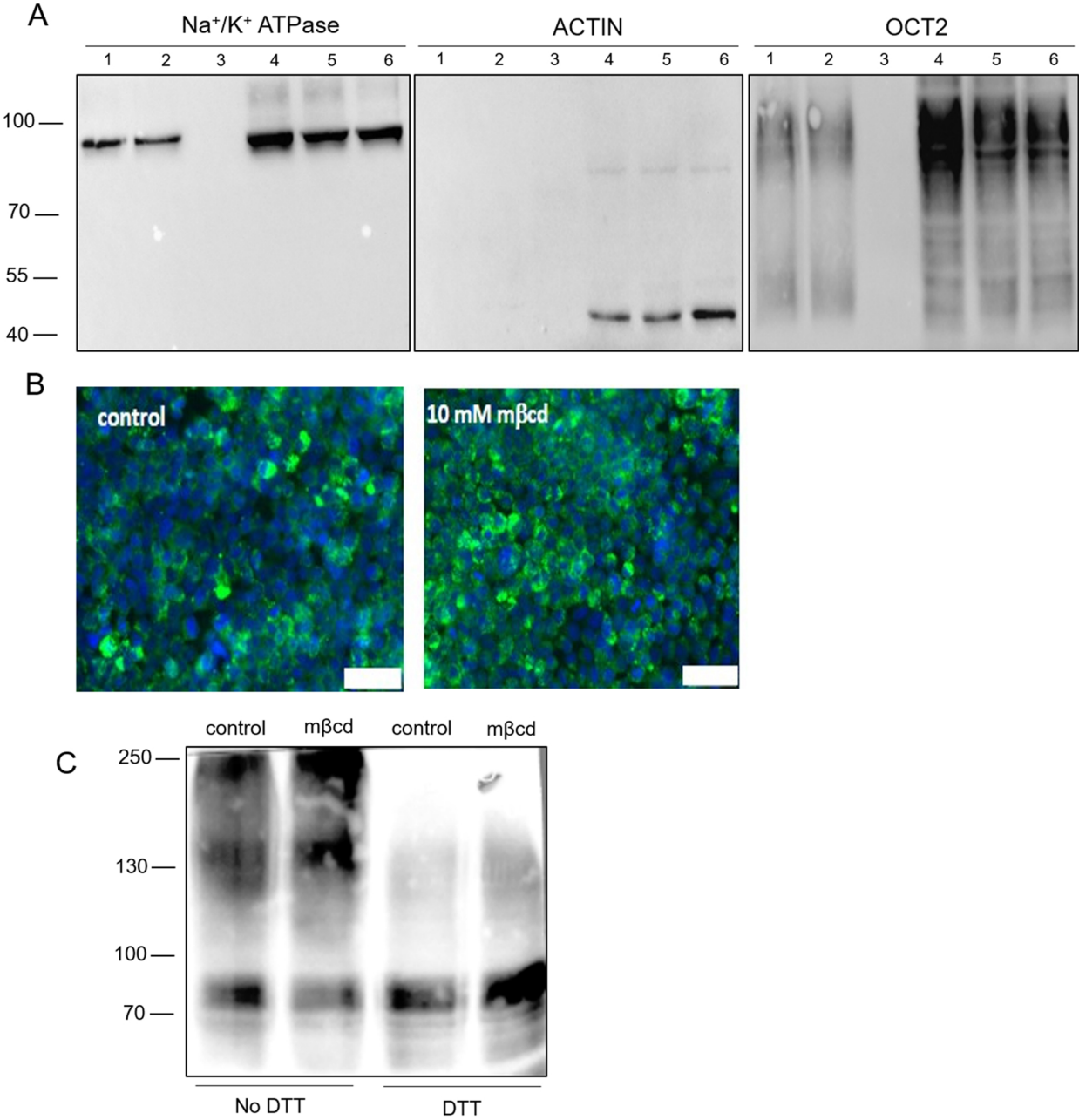


Figure 6

